Egypt. J. Chem. **Vol. 63,** No. 12 pp. 4789 - 4796 (2020)

Egyptian Journal of Chemistry

http://ejchem.journals.ekb.eg/

Modeling the Effect of Zinc Oxide on the Electronic Properties of Polyvinyl Alcohol

Rania Badry[a], Asmaa Ibrahim[b], Fatma Gamal[a], Samah A. Ibrahim[c], Hend Ezzat[d], Hanan Elhaes[a], Medhat A. Ibrahim[e]*

[a]Physics Department, Faculty of Women for Arts, Science and Education, Ain Shams University, 11757 Cairo, Egypt

[b]Basic Science Department, October High Institute for Engineering & Technology, Misr University for Science and Technology, 6th October City, Cairo, Egypt.

.[c]Physics Department, Faculty of Science, Ain Shams University, 11566 Cairo, Egypt.

[d]Nano Lab, National Research Institute of Astronomy and Geophysics (Nano NRIAG), Helwan, Cairo, Egypt

[e]Molecular Spectroscopy and Modeling Unit, Spectroscopy Department, National Research Centre, 33 El-Bohouth St., 12622, Dokki, Giza, Egypt

Abstract

A Computational study for the physical properties of polyvinyl alcohol (PVA) in its emeraldine base form (4PVA) is presented. Both PM6 semiempirical and DFT: B3LYP/LANL2DZ levels are conducted to elucidate the ZnO effects on the electronic and surface properties of PVA. The influence of ZnO was introduced in terms of total dipole moment (TDM), HOMO/LUMO band gap energy (ΔE) and molecular electrostatic potential (MESP). The results indicated that, TDM of 4PVA and ΔE were changed by changing the interaction site. Where, the band gap energy of 4PVA decreased sharply with ZnO addition and the electron density together with the reactivity was increased as presented in MESP maps. Also, the influence of ZnO addition was clearly observed from TDM and ΔE values calculated with DFT than those calculated at PM6 level. The difference between both methods could be attributed to electron correlation which is included in DFT rather than PM6, this makes DFT more accurate than PM6.

Keywords: 4PVA; ZnO; Electronic properties; Semiempirical methods; DFT: B3LYP/LANL2DZ.

1. Introduction

Since long time Zinc oxide (ZnO) is reported among the most widely material acting as metal oxide gas sensors [1-2]. ZnO could be used for detecting several gases such as hydrogen, oxygen and hydrocarbon. Sensing materials are those characterized with a change in their physical properties under the influence of the sensing gas. It is reported that, as gas interacts with ZnO surface, the surface conductivity of ZnO changes [3]. It is among the oldest known sensors, but still attracting researchers, according to its easy handling which enables its fabrication in many forms [4-5]. Better performance could be achieved with certain additives so called dopants [6-7]. Further enhancement could be achieved as it produced in nano scale, according to the huge increased in the surface area [8]. The increasing demands for preparation of metal oxides such as ZnO in nano form leads to an increase in the experimental

*Corresponding author e-mail: medahmed6@yahoo.com.; (Medhat A. Ibrahim).
Receive Date: 04 April 2020, Revise Date: 07 May 2020, Accept Date: 12 July 2020
DOI: 10.21608/EJCHEM.2020.27245.2564
©2020 National Information and Documentation Center (NIDOC)

efforts. On the other hand, theoretical approaches are also needed to follow up the changes in the electronic properties of metal oxides as a result of blending, doping and/or interaction in nano scale.
Many experimental efforts were conducted by many researchers to improve the production of ZnO in many forms mainly in nano scale [9-11]. It is reported that the sensing performance is enhanced with doping with different materials owing to the huge increase in surface area [12-13].

Beside the experimental efforts, molecular modeling with different levels of theory could be applied to metal oxides and many systems containing metal oxides in order to investigate their physical, chemical as well as surface properties [14-18]. The properties investigated by molecular modeling are considered as good indicators for reactivity of the given structure [19-24]. The modeling techniques show potential for many applications not only for sensor but also for biological as well as many applications based on the electronic properties of the investigated materials [25,26]. Among the possible blending of metal oxide is to blend with polymers such as Polyvinyl Alcohol (PVC) [27,28]. PVC is the first choice in polymer science according to its cheap price and easy handling as reported by many researchers [29-33]. It is reported that blending PVC with metal oxide enhances the properties and functionality [34-37]. Despite the various applications of PVC, some adverse impacts are reported, both pyrolysis process and thermal degradation of PVC forming chlorinated hydrocarbons, which are hazardous non-degradable and carcinogenic compounds [38, 39]. Accordingly, Polyvinyl alcohol which is abbreviated as PVA is a substituted polymer which is water-soluble has many applications [36]. However, PVA is hydrophilic [40]. The abundant hydroxyl groups allow PVA for blending which further enhance its properties [41]. PVA as well as its derivatives could be good candidate for biomedical applications [42]. Beside the well known properties of ZnO, it is reported recently that, it has a cheapest material, low toxicity, biodegradability, bio compatibility [43, 44].
Physical parameters which are calculated by molecular modeling such as total dipole moment (TDM), HOMO/LUMO band gap energy (ΔE) and molecular electrostatic potential (MESP) are considered good indicators for electronic properties and hence to the reactivity of a studied structure [45-49]. It is stated that, the reactive structure has high dipole moment while its band gap energy is low. Furthermore, one can correlate the charge distribution and the contour of the electrostatic potential with the given active sites along the surface. Finally, the parameters described with molecular modeling are correlated with the reactivity of the studied structures [50].
Based upon these considerations to functionalize Polyvinyl Alcohol it is important to tune its electronic properties in order to facilitate its applications. A metal oxide semiconductor such as ZnO could enhance the electronic properties of PVA and subsequently increases it reactivity and surface properties which could in turn enhances its ability for applications in many area. So that, this computational work is designed to elucidate the effect of ZnO upon electronic properties of PVA at semiempirical PM6 and DFT: B3LYP/LANL2DZ levels of theory.

2. Calculation Details:

All model molecules were calculated using GAUSSIAN 09 program [51], which is implemented on personal computer at Spectroscopy Department, National Research Centre (NRC), Egypt. The effect of ZnO on the electronic properties of Polyvinyl Alcohol (PVA) was studied using two different methods namely: semiempirical quantum mechanical method at PM6 level and density functional theory at DFT: B3LYP/LANL2DZ [52-54]. TDM, HOMO/LUMO band gap (ΔE) and MESP were calculated at the same level of theory.

3. Results and Discussion:

3.1. PVA Model

Before presenting the computational results it is important to describe how the model molecules were built. To build the model structure for simulating PVA, it is supposed that the model consists of four units of PVA as indicated in figure 1. For studying the interaction between PVA with ZnO, PVA belongs to the polar group of synthetic polymers, ZnO interacted with PVA only through the active sites of PVA. The proposed structure of PVA contains four active sits through the hydroxyl group (OH). The OH group was present at 4 different positions, as they were connected to carbon atoms numbered as C23, C25, C27 and C29 respectively. PVA interacts with ZnO once through O-atom and then through Zn atom. However, the

effect of ZnO on PVA can be determined at two different interaction mechanisms. Accordingly, PVA were studied and the interaction of PVA with zinc oxide in the different four active sites OH in the two odds of zinc oxide interactions as ZnO and OZn. TDM and HOMO/LUMO band gap energy were considered as perfect indicators for the determination of the electronic properties of materials. The changes occurred in the TDM and HOMO/LUMO band gap energy of all supposed models were computed at both semiempirical method at PM6 and DFT method at B3LYP using LANL2DZ basis set. Furthermore, MESP were calculated for all structures at DFT:B3LYP using LANL2DZ basis set.

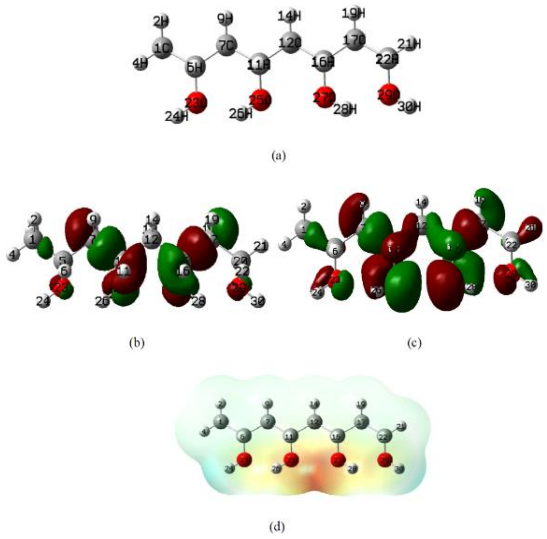

Fig. 1. Model molecule for 4PVA indicating a) Optimized structure b) PM6 calculated HOMO/LUMO band gap energy, c) DFT:B3LYP/LANL2DZ calculated HOMO/LUMO band gap energy, d) DFT:B3LYP/LANL2DZ calculated MESP as total density.

3.2. *PVA-ZnO Models*

In the first mechanism of interaction PVA interacts with ZnO throughout the zinc atom in the four OH group individually as shown in figure 2. As assumed TDM and HOMO/LUMO band gap energy for all ZnO positions with PVA computed using semiempirical method at PM6 and DFT method at B3LYP with LANL2DZ basis set. Figure 3 and 4 presented the calculated HOMO/LUMO band gap energy for the semiempirical and DFT methods respectively.

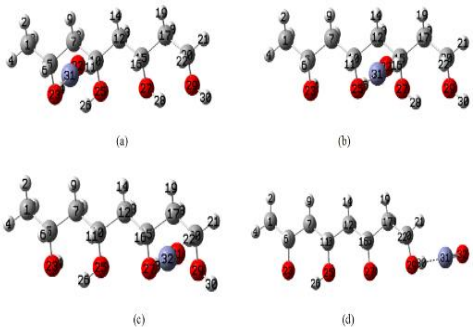

Fig. 2. DFT:B3LYP/LANL2DZ optimized structure for: a) 4PVA-(C23) ZnO b) 4 PVA-(C25) ZnO c) 4 PVA-(C27) ZnO and d) 4PVA-(C29) ZnO respectively.

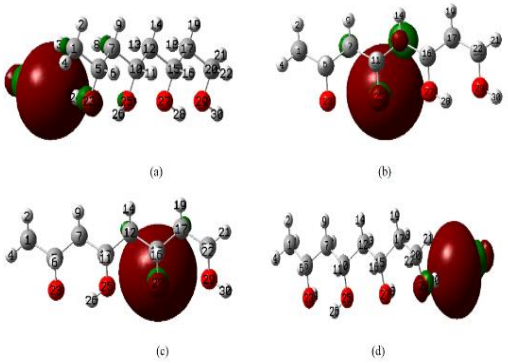

Fig. 3. PM6 calculated HOMO/LUMO band gap energy for: a) 4 PVA-(C23) ZnO b) 4PVA-(C25) ZnO c) 4 PVA-(C27) ZnO and d) 4 PVA-(C29) ZnO respectively.

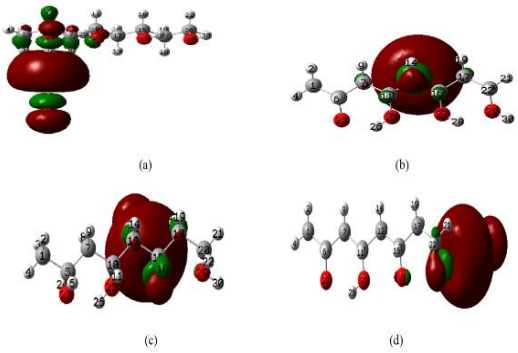

Fig. 4. DFT:B3LYP/LANL2DZ calculated HOMO/LUMO band gap energy for: a) 4 PVA-(C23) ZnO b) 4 PVA-(C25) ZnO c) 4 PVA-(C27) ZnO and d) 4 PVA-(C29) ZnO respectively.

TDM and HOMO/LUMO band gap energy listed in table 1 and table 2 respectively for the two calculations of four OH positions with ZnO using semiempirical method and DFT methods. TDM of the base PVA using semiempirical method was 5.7115 Debye , while with DFT it becomes 8.1463

Debye. In the case of 4PVA interacted with ZnO in the four actives OH positions via C23, C25, C27 and C29, TDM with semiempirical method was found to be 10.5364, 9.3974, 9.6539 and 8.5410 Debye respectively. Meanwhile for DFT method, TDM was 9.8964, 8.4196, 8.8414 and 7.9202 Debye for the same sequence.

The changes in ΔE of 4PVA and 4PVA interacted with ZnO are presented in table 2. As indicated, the values of 4PVA HOMO/LUMO energy calculated using PM6 and B3LYP/LANL2DZ were 11.9200 and 3.1058eV respectively. However, the HOMO/LUMO band gap energy for 4PVA interacted with ZnO throughout C23, C25, C27 and C29 calculated using PM6 becomes 5.1599, 5.2586, 5.3759 and 5.0932 eV respectively, while for B3LYP/ LANL2DZ becomes 1.8493, 2.3429, 2.5729 and 1.7288 eV.

Generally, the results indicated that the addition of ZnO affects positively on the electronic properties of PVA. TDM increased slightly at both methods: semiempirical and DFT while, HOMO/LUMO band gap energy sharply deceased as a result of ZnO addition. From table 1, it is clear that the differences in the TDM values calculated at semiempirical and DFT methods were noticeable but not very large. On the other hand and as presented in table 2, there was a significant difference in the values of ΔE between the two quantum mechanical methods. Therefore, for the first interaction mechanism, the results indicated that the semiempirical computed values cannot be compared with those obtained using DFT method. PM6 is not provided with electron correlation rather than DFT which gave an advantage for DFT. Accordingly, DFT method at B3LYP utilizing LANL2DZ basis set is suitable for studying the electronic properties of synthetic polymers as well as polymers interacted with ZnO.

Table 1. Calculated total dipole moment (TDM) as Debye at PM6 semiempirical level and at DFT:B3LYP/LANL2DZ for PVA and PVA/ZnO interacted through Zn atom.

Structure	TDM	
	PM6	DFT
4PVA	5.7115	8.1463
4 PVA-(C23) ZnO	10.5364	9.8964
4 PVA-(C25) ZnO	9.3974	8.4196
4 PVA-(C27) ZnO	9.6539	8.8414
4 PVA-(C29) ZnO	8.5410	7.9202

Table 2. Calculated HOMO/LUMO band gap energy(ΔE) as eV at PM6 semiempirical level and DFT:B3LYP/LANL2DZ for PVA and PVA/ZnO interacted through Zn atom.

Structure	ΔE	
	PM6	DFT
4PVA	11.9200	3.1058
4PVA-(C23) ZnO	5.1599	1.8493
4 PVA-(C25) ZnO	5.2586	2.3429
4 PVA-(C27) ZnO	5.3759	2.5729
44PVA-(C29) ZnO	5.0932	1.7288

3.3. *PVA-OZn Model*

Second interaction mechanism was presented such that PVA interacts with ZnO throughout the oxygen atom in the four OH group individually as shown in figure 5. Additionally, TDM and HOMO/LUMO band gap energy for all OZn positions with PVA calculated with semiempirical method at PM6 and with DFT method at B3LYP using LANL2DZ basis set. Figures 6 and 7 introduce calculated HOMO/LUMO band gap energy for the semiempirical method and DFT method respectively.

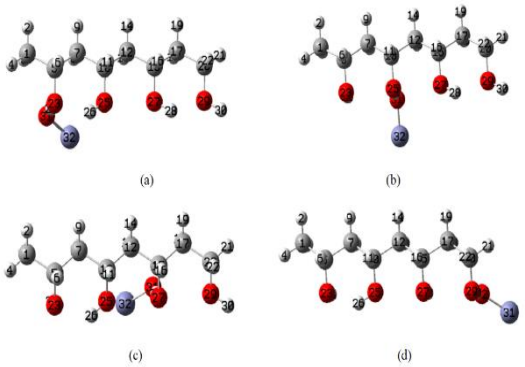

Fig. 5. DFT:B3LYP/LANL2DZ optimized structure for: a) 4 PVA-(C23) OZn; b) 4 PVA-(C25) OZn; c) 4PVA-(C27) OZn and d) 4 PVA-(C29) OZn respectively.

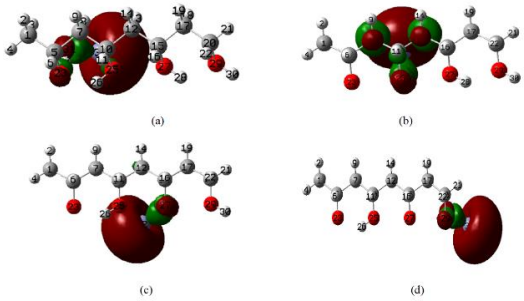

Fig. 6. PM6 calculated HOMO/LUMO band gap energy for: a) 4PVA-(C23) OZn; b) 4 PVA-(C25) OZn; c) 4 PVA-(C27) OZn and d) 4 PVA-(C29) OZn respectively.

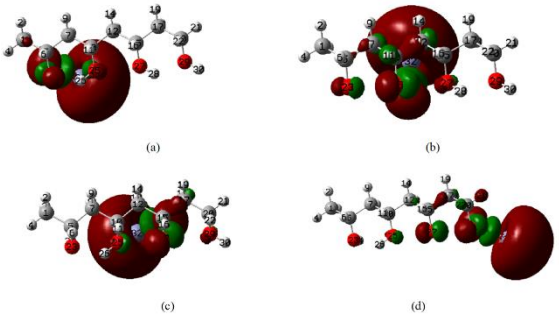

Fig. 7. DFT:B3LYP/LANL2DZ calculated HOMO/LUMO band gap energy for: a) 4PVA-(C23) OZn; b) 4 PVA-(C25) OZn; c) 4 PVA-(C27) OZn and d) 4PVA-(C29) OZn respectively.

Table 3 presents the second interaction mechanism of 4PVA with ZnO through the four different OH active groups throughout the O atom, TDM of 4PVA using semiempirical method at PM6 becomes 5.2826, 3.5467, 6.0338 and 6.4774 Debye for 4PVA interacted with OZn via C23, C25, C27 and C29 respectively, while for DFT method, TDM became 6.8035, 2.6914, 5.1594 and 5.4784 Debye. This means that the two mechanisms of interaction follow the same behavior as the changes in TDM values were small. Meanwhile, HOMO/LUMO band gap ΔE of 4PVA interacted with (Cx) OZn, table 4 confirmed that the electronic band gap for all structures calculated with both semiempirical method and DFT method was sharply decreased. ΔE decreased to 5.4657, 4.4077, 4.1835 and 5.0265 eV with semiempirical method and to 1.2667, 0.9377, 1.0618 and 0.6944 eV with DFT for 4 PVA-(C23) OZn, 4 PVA-(C25) OZn, 4 PVA-(C27) OZn and 4 PVA-(C29) OZn respectively. The calculated values of TDM and ΔE obtained at the higher level of theory (B3LYP/LANL2DZ) were more accurate than the semiempirical ones. This could be attributed to the effect of electron correlation which is implemented in DFT method.

Table 3. Calculated total dipole moment (TDM) as Debye at PM6 semiempirical level and at DFT:B3LYP/LANL2DZ for PVA and PVA/ZnO through O atom.

Structure	TDM	
	PM6	DFT
4 PVA-(C23) OZn	5.2826	6.8035
4PVA-(C25) OZn	3.5467	2.6914
4PVA-(C27) OZn	6.0338	5.1594
4 PVA-(C29) OZn	6.4774	5.4784

Table 4. Calculated HOMO/LUMO band gap energy(ΔE) as eV at PM6 semiempirical level and at DFT:B3LYP/LANL2DZ for PVA and PVA/ZnO through O atom of ZnO.

Structure	ΔE	
	PM6	DFT
4 PVA-(C23) OZn	5.4657	1.2667
4 PVA-(C25) OZn	4.4077	0.9377
4 PVA-(C27) OZn	4.1835	1.0618
4 PVA-(C29) OZn	5.0265	0.6944

3.4. *Molecular Electrostatic Potential (MESP)*

Another important electronic (surface) descriptor was calculated for 4PVA as well as 4PVA/ZnO is the molecular electrostatic potential (MESP). MESP illustrates the distribution of electronic charges of molecules within the studied structures in three dimensions. Also, MESP could be presented as color mapped surfaces ranging from red to blue. The red color refers to the most negative regions (i.e. the regions very rich with electrons) while, the blue one refers to the most positive one (i.e. the regions These color maps help in visualizing properties of molecules such as shape, size and the complex structures behavior. To predict the interaction nature whether it nucleophilic or electrophilic, the MESP was calculated for 4PVA proposed structure at the DFT:B3LYP/LANL2DZ level. The MESP maps for 4PVA were presented in figures 8 and 9. As presented in the figures, that the maximum negative MESP was located at the oxygen atom of PVA and that of metal oxide (i.e. C-O and Zn-O bonds) referring to an electrophilic interaction. Meanwhile, the most positive MESP was located at the carbon and hydrogen atoms (i.e. C-H bond) which refers to a suitable site for a nucleophilic attack. Generally, the MESP results confirmed the results of HOMO/LUMO band gap ΔE for all the studied structures, where the reactivity of the studied model molecules increased due to the interaction with zinc oxide molecule.

In this sense the interaction between ZnO and PVA weather the interaction took place through O and/or Zn atoms leads to an enhancement of the surface properties. This dedicates that the studied PVA/ZnO as well as PVA/OZn are suitable structures for applications gas sensor according to their unique surface active sites induced as a result of ZnO.

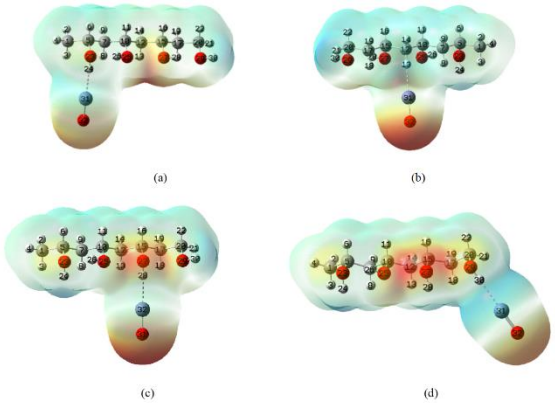

Fig. 8. DFT:B3LYP/LANL2DZ calculated MESP as total density for: a) 4PVA-(C23) ZnO; c) 4 PVA-(C25) ZnO; d) 4 PVA-(C27) ZnO and e) 4 PVA-(C29) ZnO respectively.

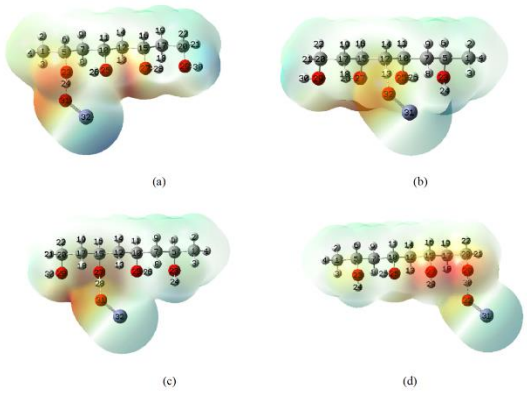

Fig. 9. DFT:B3LYP/LANL2DZ calculated MESP as total density for: a) 4 PVA-(C23) OZn; b) 4 PVA-(C25) OZn; c) 4 PVA-(C27) OZn and d) 4 PVA-(C29) OZn respectively.

4. Conclusion:

This computational work presents the electronic properties of PVA using two methods namely DFT:B3LYP/LANL2DZ and PM6. The changes in the electronic properties of PVA were discussed in terms of TDM, HOMO/LUMO band gap energy ΔE and MESP. The calculated HOMO/LUMO band gap ΔE with PM6 semiempirical method shows that the results are not comparable with that calculated with DFT:B3LYP/LANL2DZ. It could be concluded that, the computational methods could describe both surface and electronic properties of polymers as well as polymer interacted with metal oxides. Moreover, the electron correlation which is included in DFT: B3LYP/LANL2DZ methods gives it advantages in comparison with semiempirical method such as PM6. In spite of this, PM6 could be useful to provide comparable results in appropriate computational times. Enhancement of the electronic properties of PVA as indicated by the calculated physical parameters dedicate it for many applications based on its surface activity such as sensor. This in turn could produce cost effective sensor based on the investigated properties in one hand and on the low cost and easy handling of PVA on the other hand.

5. References:

[1] Ried R. P., Kim E., Hong D. M. and Muller R. S., Piezoelectric microphone with on-chip CMOS circuits, Journal of Microelectromechanical Systems, 2(3), 111-120 (1993)

[2] Ito Y., Kushida K., Sugawara K. and Takeuchi H., A 100-Mhz ultrasonic transducer array using ZnO thin films, IEEE Transaction on Ultrasonics, Ferroelectrics, and Frequency Control,42(2), 316-323 (1995).

[3] Heiland G., Homogeneous semiconducting gas sensors, Sensors and Actuators, 2, 343-361(1982).

[4] Dong L. F, Cui Z. L. and Zhang Z. K., Gas sensing properties of nano-ZnO prepared by arc plasma method, Nanostructured Materials, 8(7), 815-823 (1997).

[5] Basu S. and Dutta A., Room-temperature hydrogen sensors based on ZnO, Materials Chemistry and Physics, 47(1), 93-96 (1997).

[6] Nanto H., Sokooshi H., and Usuda T., Smell sensor using aluminium-doped zinc oxide thin film prepared by sputtering technique, Sensors and Actuators, B. 10(2), 79-83 (1993).

[7] Inoue K. and Miyayama M., Chlorine Gas Sensing Properties of ZnO-CaO Ceramics, Journal of Electroceramics, 2, 41-48 (1998).

[8] Bott B., Jones T. A. and Mann B., The detection and measurement of CO using ZnO single crystals, Sensors and Actuators, 5(1), 65-73 (1984).

[9] Jones A., Jones T. A., Mann B. and Firth J. G., The effect of the physical form of the oxide on the conductivity changes produced by CH4, CO and H2O on ZnO, Sensors and Actuators, 5(1), 75-88 (1984).

[10] Mitra P., Chatterjee A. P., and Maiti H. S., ZnO thin film sensor, Materials Letters, 35(1-2), 33-38 (1998).

[11] Xu J., Pan Q., Shun Y., and Tian Z., , Grain size control and gas sensing properties of ZnO gas sensor, Sensors and Actuators B: Chemical, 6(1-3) 277-279 (2000).

[12] Nanto H., Minami T., and Takata S., Zinc-oxide thin-film ammonia gas sensors with high sensitivity and excellent selectivity, Journal of Applied Physics, 60(2), 482-484 (1986)

[13] Mukhopadhyay A. K., Mitra P., Chattopadhyay D., and Maiti H. S., Influences of fabrication techniques and doping on hydrogen sensitivity of zinc oxide sensors, Journal of Materials Science Letters,15, 431-433 (1996).

[14] Elhaes H., Fakhry A. and Ibrahim M., Carbon Nano Materials as Gas Sensors, Materials Today: Proceedings, 3(6), 2483-2492 (2016).

[15] Ibrahim M. A., Elhaes H., El-Khodary S. A., Morsy M., Refaat A., Yahia I. S. and Zahran H. Y., Molecular Modeling Analyses for the Effect of Alkali Metal Oxides on Graphene, Biointerface Research in Applied Chemistry, 8, 3522-3525 (2018).

[16] Ezzat H. A., Hegazy M.A., Nada N. A. and Ibrahim M. A., Effect of Nano Metal Oxides on the Electronic Properties of Cellulose, Chitosan and Sodium Alginate , Biointerface Research in Applied Chemistry, 8 (4), 4143-4149 (2019).

[17] Ezzat H. A., Hegazy M. A., Nada N. A., Osman O., Ibrahim M. A., Application of Natural Polymers Enhanced with ZnO and CuO as Humidity Sensor, NRIAG Journal of Astronomy and Geophysics, 9, 586-597(2020).

[18] Sabry N. M., Tolba S., Abdel-Gawad F. Kh., Bassem S. M., Nassar H., El-Taweel G. E. and Ibrahim M., On the Molecular Modeling Analyses of the Interaction between Nano Zinc Oxide and Bacteria, Biointerface Research in Applied Chemistry, 8 (3), 3294 – 3297 (2018).

[19] Alghunaim N. S., Omar A., Elhaes H. and Ibrahim M., Effect of ZnO and TiO2 On the Reactivity of Some Polymers, Journal of Computational and Theoretical Nanoscience, 14, 2838–2843 (2017).

[20] Refaat A., Youness R. A., Taha M. A., Ibrahim M., Effect of Zinc Oxide on the Electronic Properties of Carbonated Hydroxyapatite, Journal of Molecular Structure, 1147, 148-154 (2017).

[21] Menazea A. A., Ezzat H. A., Omara W., Basyouni O. H., Ibrahim S. A., Mohamed A. A., Tawfik W., Ibrahim M. A., Chitosan/graphene oxide composite as an effective removal of Ni, Cu, As, Cd and Pb from wastewater, 1189 ,112980, Computational and Theoretical Chemistry, (2020).

[22] Badry R., Ibrahim A., Gamal F., Shehata D., Ezzat H., Elhaes H., Ibrahim M., Electronic Properties of Polyvinyl alcohol/ TiO_2/SiO_2 Nanocomposites, Biointerface Research of Applied Chemistry, 10, 6427-6435,(2020).

[23] Ghasemi A.; Fazaeli R.; Ghiasi, R., DFT and NBO Studies of Stability, Electronic, and Structural Features of the 2-fluoroacetaldehyde Conformers, Egyptian Journal of Chemistry, 63, 315-324 (2020)

[24] Ezzat H. A., Gomaa I., Gawad A. El-D. A., Osman O., Mahmoud A. A., Sleim M., Elhaes H., Ibrahim M. A., Semiempirical Molecular Modeling Analyses for Graphene/Nickel Oxide Nanocomposite, Letters in applied NanoBioScince. 9, 1459 – 1466, (2020).

[25] Bayoumy A. M., Elhaes H., Osman O., Hussein T. and Ibrahim M. A., Mapping Molecular Electrostatic Potential for Heme Interacting with Nano Metal Oxides, Biointerface Research in Applied Chemistry, 10(2), 5091 – 5095 (2020).

[26] Bayoumy A. M., Elhaes H., Osman O., Kholmurodov Kh. T., Hussein T. and Ibrahim M. A., Effect of Nano Metal Oxides on Heme Molecule: Molecular and Bimolecular Approaches, Biointerface Research in Applied Chemistry, 10(1), 4837-4845 (2020).

[27] Refaat A., Ibrahim M. A., Elhaes H., Badry R., Ezzat H., Yahia I. S., Zahran H. Y. and Mohd. Shkir, Geometrical, vibrational, and physical properties of polyvinyl chloride nanocomposites: Molecular Modeling Approach A companied molecular modeling and FTIR spectroscopy, Journal of theoretical and computational chemistry, 18(8),1950037(2019).

[28] D'Aquino W, Balmant, C. A., Ribeiro R. L. L., Munaro M., Vargas J.V.C. and Amico S.C., A simplified mathematical model to predict PVC photodegradation in photobioreactors, Polymer Testing, 31(5), 638-644 (2012).

[29] Al-Malack H. M., Migration of lead from unplasticized polyvinyl chloride pipes, Journal of Hazardous Materials, 82(3), 263-274 (2001).

[30] Rajendran S. and Uma T., Effect of ZrO2 on conductivity of PVC–LiBF4–DBP polymer electrolytes, Materials Letters, 44(3-4), 208-214(2000).

[31] Sun H., Cao B., Tian Q., Liu S., Du D., Xue Z. and Fu H., A DFT study on the absorption mechanism of vinyl chloride by ionic liquids, Journal of Molecular Liquids, 215, 496 - 502(2016).

[32] Brydson J. A., Plastics Materials, 6th Edition. Butterworth-Heinemann, USA. (1995).

[33] Chopra S., Electronic properties and optical absorption of graphene-polyvinylidene fluoride nanocomposites:A theoretical study, Materials Chemistry and Physics, 186,159-166(2017).

[34] Mallakpour S. and Shafiee E., The synthesis of poly(vinyl chloride) nanocomposite films containing ZrO2 nanoparticles modified with vitamin B1 with the aim of improving the mechanical, thermal and optical properties. Des Monomers Polym. , 20(1), 378-388(2017).

[35] Hoherčáková Z. and Opekar F., Au/PVC composite a new material for solid-state gas sensors: Detection of nitrogen dioxide in the air, Sensors and Actuators B: Chemical, 97(2-3), 379- 386(2004).

[36] Hu J., Zhu Y., Huang H. and Lu J., Recent advances in shape–memory polymers: Structure, mechanism, functionality, modeling and applications, Progress in Polymer Science, 37(12), 1720-1763(2012).

[37] McNeill I.C., Memetea L. and Cole W.J. A study of the products of PVC thermal degradation, Polymer Degradation and Stability, 49(1),181–191(1995).

[38] Czégény Z., Jakab E., Blazsó M., Bhaskar T. and Sakata Y., Thermal decomposition of polymer mixtures of PVC, PET and ABS containing brominated flame retardant: formation of chlorinated and brominated organic compounds, Journal of Analytical and Applied Pyrolysis, 96,69–77(2012).

[39] Kulesza K. and German K. Chlorinated pyrolysis products of co-pyrolysis of poly(vinyl chloride) and poly(ethylene terephthalate), Journal of Analytical and Applied Pyrolysis, 67, 123–134(2003).

[40] Dai H., Huang Y. and Huang H., Eco-friendly polyvinyl alcohol/carboxymethyl cellulose hydrogels reinforced with graphene oxide and bentonite for enhanced adsorption of methylene blue, Carbohydrate Polymers, 185, 1-11(2018).

[41] Schellekens R. and Bastiaansen C., The drawing behavior of polyvinylalcohol fibers, Journal of Applied Polymer Science, 43 (12), 2311-2315(1991).

[42] Rudra R., Kumar V. and Kundu P.P., Acid catalysed cross-linking of poly vinyl alcohol (PVA) by glutaraldehyde: Effect of crosslink density on the characteristics of PVA membranes used in single chambered microbial fuel cells, Royal Society of Chemistry Advances, 5 (101), 83436-83447 (2015).

[43] Paralikar S.A., Simonsen J. and Lombardi J., Poly(vinyl alcohol)/cellulose nanocrystal barrier membranes Journal of Membrane Science, 320(1–2), 248-258(2008).

[44] Yadav R., Muralidhar A., Shamna A., Aghila P., Gurrala L. and Sakthivel A., Aluminium Oxide Supported on SBA-15 Molecular Sieves as Potential Lewis Acid Catalysts for Epoxide Ring Opening Using Aniline, Catalysis Letters, 148(5), 1407-1415(2018).

[45] Ibrahim M. and El-Haes H., Computational Spectroscopic Study of Copper, Cadmium, Lead and Zinc Interactions in the Environment, International Journal of Environment and Pollution, 23(4), 417-424(2005).

[46] Ibrahim M., Molecular Modelling and FTIR Study for K, Na, Ca and Mg Coordination with Organic Acid, Journal of Computational and Theoretical Nanoscience, 6(3), 682–685(2009).

[47] M. Ibrahim and Mahmoud A-A., Computational Notes on the Reactivity of some Functional Groups, Journal of Computational and Theoretical Nanoscience, 6(6), 1523–1526(2009).

[48] Ali G.W., Abdel-Fattah W.I., Elhaes H. and Ibrahim, M.A., Spectroscopic and modeling analyses of bimolecular

structure of corn silk. Biointerface Research in Applied Chemistry, 9, 4581–4585 (2019).
[49] Politzer P., Laurence P.R. and Jayasuriya K., Molecular electrostatic potentials: an effective tool for the elucidation of biochemical phenomena. Environmental Health Perspectives, 61, 191–202(1985).
[50] Şahin Z.S., Şenöz H.I., Tezcan H. and Büyükgüngör O., Synthesis, spectral analysis, structural elucidation and quantum chemical studies of (E)-methyl-4-[(2-phenylhydrazono)methyl]benzoate, Spectrochimica Acta Part A: Molecular and Biomolecular Spectroscopy, 143, 91–100(2015).
[51] Frisch M. J. et al. Gaussian, Inc., Wallingford CT, 2010.
[52] Becke A. D., Density-functional thermochemistry. III. The role of exact exchange. The Journal of Chemical Physics, 98, 5648–5652(1993).
[53] Lee C., Yang W. and Parr R.G., Development of the Colic-Salvetti correlation-energy formula into a functional of the electron density, Physical Review B, 37, 785(1988).
[54] Miehlich B., Savin A., Stoll H and Preuss H., Results obtained with the correlation energy density functionals of Becke and Lee, Yang and Parr, Chemical Physics Letters,157(3), 200-206(1989).